Is Slow Slip in Subduction Zones for Real?

Jyoti Behura[1] and Farnoush Forghani[2]

[1]Seismic Science LLC
[2]University of Colorado

November 21, 2022

Abstract

The Slow-Slip hypothesis is postulated on two observations– existence of tectonic tremors and their spatio-temporal correlation with anomalous slow reversals in horizontal geodetic measurements. The above observations have led geoscientists to believe that the down-dip portion of the plate interface is slowly shearing and releases energy gradually in the form of tremor. However, numerous observations and scientific findings are poorly explained by the Slow-Slip hypothesis. Here, we show that periodic seismic activity and geodetic changes, result from the episodic buckling of the overriding continental crust and its rapid collapse on the subducting oceanic slab. According to the Episodic Buckling and Collapse hypothesis, geodetic measurements, previously inferred as slow slip, are the surficial expressions of slowly-evolving buckling and rapid collapse of the over-riding plate, while tremor swarms result from the striking of the collapsing overriding plate on the subducting slab (as opposed to slipping or shearing).

Is Slow Slip in Subduction Zones for Real?

Jyoti Behura[1,2] and Farnoush Forghani[3]

[1]Colorado School of Mines
[2]Seismic Science LLC
[3]University of Colorado, Anschutz Medical Campus

Key Points:

- Numerous observations and scientific findings are poorly explained by the Slow-Slip model of subduction zones
- By employing all existing observations, we develop an Episodic Buckling and Collapse model of the subduction zone, wherein the overriding continental crust buckles upwards and landwards because of compressive stress from the subducting slab, and then collapses on the slab as fluid pressure in the LVZ is released
- Geodetic measurements, previously inferred as slow slip, are the surficial expressions of slowly-evolving buckling, while the relatively short-lived tremor results from the striking of the rapidly collapsing overriding plate on the subducting slab
- Proposed subduction zone model has major implications for forecasting of megathrust earthquakes and for magma transport from the mantle to the crust

Corresponding author: Jyoti Behura, `jbehura@mines.edu`

Abstract

The Slow-Slip hypothesis is postulated on two observations existence of tectonic tremors and their spatio-temporal correlation with anomalous slow reversals in horizontal geodetic measurements. The above observations have led geoscientists to believe that the down-dip portion of the plate interface is slowly shearing and releases energy gradually in the form of tremor. However, numerous observations and scientific findings are poorly explained by the Slow-Slip hypothesis. Here, we show that periodic seismic activity and geodetic changes, result from the episodic buckling of the overriding continental crust and its rapid collapse on the subducting oceanic slab. According to the Episodic Buckling and Collapse hypothesis, geodetic measurements, previously inferred as slow slip, are the surficial expressions of slowly-evolving buckling and rapid collapse of the overriding plate, while tremor swarms result from the striking of the collapsing overriding plate on the subducting slab (as opposed to slipping or shearing).

Plain Language Summary

Nearly a couple of decades ago, geoscientists discovered interesting deep seismic events in subduction zones (which they termed tectonic tremor) and found that these phenomena had a strong spatio-temporal correlation with surficial displacements. This remarkable spatio-temporal correlation led them to postulate the slow-slip hypothesis wherein a part of the continental-oceanic interface shear slowly over a few days or weeks (as opposed to conventional earthquakes that span a few seconds). However, numerous observations and findings are poorly explained by the slow-slip hypothesis. We employ all existing observations and research to develop the Episodic Buckling and Collapse model of the subduction process. We show that tremor and surficial displacements, previously associated with so-called "slow slip", in fact result from the episodic buckling of the overriding continental crust and its rapid collapse on the subducting oceanic slab.

1 Tectonic Tremor, Slow Slip, and their Episodic Nature

Obara (2002) observed non-impulsive "noisy" records on Hi-net seismograms in southwest Japan. Such seismic records, commonly referred to as tectonic tremors (or non-volcanic tremors), are different from impulsive earthquakes as well as volcanic tremors. Tectonic tremors may last for hours, days, or weeks at a stretch (Wech et al., 2009; Beroza & Ide, 2011). More interestingly, tectonic tremors are episodic as first reported by Obara (2002) – they repeat with near clock-like regularity. In the Nankai subduction zone, the periodic interval between two consecutive tremor episodes varies between 3 and 9 months (Obara, 2011; Obara et al., 2011, 2012), while in Cascadia, the interval ranges between 12 and 15 months. Moreover, within each tremor episode, the tremor migrates up-dip (Shelly et al., 2007; Wech et al., 2009; Ghosh et al., 2010; Obara et al., 2012) as well as along-strike of the plate interface (Shelly et al., 2007; Wech et al., 2009; Obara et al., 2012).

During the same period, scientists also discovered reversals on horizontal GPS records (Hirose et al., 1999; Dragert et al., 2001) lasting several days that they attributed to slow-slip along the interface between the overriding and subducting plates. Subsequently, Miller et al. (2002) reported that these slow earthquakes in Cascadia occurred nearly periodically every 14.5 months. In a major development, Rogers and Dragert (2003) discovered that the periodic slow earthquakes in Cascadia observed by Miller et al. (2002) coincide with tectonic tremor, both temporally and spatially. They termed this phenomenon Episodic Tremor and Slip (ETS). Thereafter, Obara et al. (2004) also observed the presence of ETS in the Nankai subduction zone in Japan. However, instead of GPS, Obara et al. (2004) employed tiltmeter records where they observed anomalies in surface tilt also coinciding temporally and spatially with tectonic tremor activity. Scientists also use the term Slow-Slip instead of ETS to emphasize that tremor and slip are the same phenomenon.

Existing hypotheses on physical processes explaining slow-slip and tremors are well summarized by J. Gomberg (2010), Beroza and Ide (2011), and Vidale and Houston (2012). The mechanics of slow-slip, tremors and their periodic nature, however, is a topic of intense debate among seismologists and remains largely unresolved because of the lack of adequate explanation of multiple physical phenomena and scientific findings using the Slow-Slip hypothesis. We elucidate some of these discrepancies below.

Here, we present a model of the subduction process developed by utilizing all the existing geodetic observations, imaging studies, geologic inferences, seismological analysis, and previously unused geodetic data. According to this model, geodetic observations previously interpreted as slow slip, are in fact a surface manifestation of the buckling of the overriding continental crust and its subsequent rapid collapse on top of the subducting oceanic slab. The said collapse-related striking of the continental crust on the subducting slab results in tremors and the collapse itself shows up as rapid reversals in the horizontal GPS component. The proposed subduction model has significant and direct implication for forecasting of megathrust earthquakes and provides a 'breathing' mechanism for the upwelling and flow of magma from the mantle to the shallow crust. A preliminary version of this model was initially proposed in Behura et al. (2018) and has been modified here.

2 Published Observations and Findings

Table 1 summarizes various geodetic observations, seismological studies, imaging research, and geologic findings, all of which should provide constraints for any model of the subduction zone. In addition, Table 1 summarizes how these observations fit the two subduction zone models – the Slow-Slip and the Episodic Buckling and Collapse hypotheses. Thereafter, in section 3, we use these observations to develop the Episodic Buckling and Collapse model and explain how other scientific findings are reasonably explained by it.

2.1 Geodetic Observations

In addition to the reversals in horizontal GPS recordings, similar and more prominent reversals are observed on the vertical GPS component (Douglas, 2005; Miyazaki et al., 2006; Heki & Kataoka, 2008; Behura et al., 2018). Magnitude of the vertical displacements cannot be satisfactorily explained by the Slow-Slip hypothesis as it assumes only relative sliding between the subducting slab and the overriding plate.

Tiltmeter recordings (Obara et al., 2004; Hirose & Obara, 2005, 2010) show significant bulging of the surface prior to slow slip and subsequent contraction coinciding with slow slip. Although temporal changes in tiltmeter recordings can be resonably explained by the Slow-Slip hypothesis, accounting for the spatial changes through slow slip is more challenging.

2.2 Fluids and the Low-Velocity Zone

Numerous studies (Eberhart-Phillips et al., 2006; Matsubara et al., 2009; Audet et al., 2009; Bell et al., 2010; Toya et al., 2017) clearly demonstrate the presence of fluids at the plate interface characterized by a seismic Low-Velocity Zone (LVZ). It is widely believed that slab dehydration generates aqueous fluids which then travel upward because of buoyancy forces and accumulate at the plate interface and mantle wedge. Seismologists believe that these fluids lubricate the plate interface thereby aiding slow slip and aseismic slip.

In Cascadia, evidence of fluids come from the work of (Audet et al., 2009) who employ teleseismic data to show the presence of a zone with anomalously high Poisson's ra-

Observations	**Slow-Slip**	**EBC**	**References**
GPS Horizontal	✓	✓	(Hirose et al., 1999; Dragert et al., 2001)
GPS Vertical	✗	✓	(Douglas, 2005; Miyazaki et al., 2006; Heki & Kataoka, 2008; Behura et al., 2018)
Tiltmeter recordings	✓(?)	✓	(Obara et al., 2004; Hirose & Obara, 2005, 2010)
Presence of fluids in LVZ	✓	✓	(Eberhart-Phillips et al., 2006; Matsubara et al., 2009; Audet et al., 2009; Bell et al., 2010; Toya et al., 2017)
Large fluid pressure in LVZ	✓(?)	✓	(Audet et al., 2009; Toya et al., 2017)
Low effective stress	✗	✓	(Rubinstein et al., 2007; Bell et al., 2010)
Episodic fluid drainage	✗	✓	(Nakajima & Uchida, 2018)
Thick LVZ	✓(?)	✓	(Toya et al., 2017; Audet & Schaeffer, 2018)
LVZ Geometry and their up-dip & down-dip extents	✓(?)	✓	(Hansen et al., 2012; Toya et al., 2017; Audet & Schaeffer, 2018)
Occurrence of tremors	✓	✓	(Obara, 2002)
Tremor source mechanism	✓(?)	?	(Shelly et al., 2006; Wech & Creager, 2007; Ide et al., 2007; Bostock et al., 2012; K. Ohta et al., 2019)
Spatial extent of tremors	✓(?)	✓	(Wech et al., 2009; Kao et al., 2009; Audet et al., 2010; Audet & Schaeffer, 2018)
Tremor migration patterns	✗	✓	(Shelly et al., 2007; Wech et al., 2009; Kao et al., 2009; Ghosh et al., 2010; Boyarko & Brudzinski, 2010; Obara et al., 2011, 2012)
Tremor migration reversals	✗	✓	(Houston et al., 2011; Obara et al., 2012)
Absence of tremors on old crusts	✗	✓	(Schwartz & Rokosky, 2007)
Variable tremor and slow slip periodicity	✗	✓	(Wallace & Beavan, 2010)
Tremors located down-dip of LVZ	✗	✓	(Peterson & Christensen, 2009; Audet & Schaeffer, 2018)
Crustal seismicity	✗	✓	(Nicholson et al., 2005; Shelly et al., 2006; Bostock et al., 2012)
Mantle helium correlation with tremor location	✓(?)	✓	(Umeda et al., 2007; Sano et al., 2014)
Paleo-uplift and subsidence	✗	✓	(Dragert et al., 1994; Sherrod, 2001; Leonard et al., 2004; Shennan & Hamilton, 2006)

Table 1: List of observations and results used in constructing the Episodic Buckling and Collapse model of subduction zones. Symbols ✓ correspond to an adequate explanation of the observation provided by a theory, while ✗ represents the lack of a reasonable explanation. Hypothesis that have been proposed to explain observations but have significant drawbacks are denoted by the symbol ✓(?), while **?** is used when no study exists.

tio extending from the margin all the way to the corner of the mantle wedge. Presence of fluids in the tremor region in Shikoku is evident from the tomographically-derived low velocities by (Shelly et al., 2006) and (Matsubara et al., 2009).

Other studies show that the plate interface is overpressured (Audet et al., 2009; Toya et al., 2017). (Rubinstein et al., 2007; Bell et al., 2010) find extremely low effective normal stresses in subduction zones. Excepting buoyancy recharging the plate boundary with hydrous magmatic fluids, the Slow-Slip model provides little explanation of the cause of overpressure and their periodic nature.

Recent findings by Nakajima and Uchida (2018) shed new light on the movement of fluids at the plate boundary. They analyze seismic data spanning more than a decade over Japan and demonstrate that "seismicity rates and seismic attenuation above the megathrust of the Philippine Sea slab change cyclically in response to accelerated slow slip." They interpret these findings to represent "intensive drainage during slow slip events that repeat at intervals of approximately one year and subsequent migration of fluids into the permeable overlying plate." Although Nakajima and Uchida (2018) provide an explanation of these observation in the context of the Slow-Slip hypothesis, it is unclear what forces drive the fluids in and out of the plate boundary.

The spatial extent and geometry of the LVZ are clear from the work of Hansen et al. (2012); Toya et al. (2017); Audet and Schaeffer (2018). Toya et al. (2017); Audet and Schaeffer (2018) report a thick LVZ with thicknesses averaging a few kilometers in the Cascadia Subduction Zone. All of them also report the thickening of the LVZ with increasing depth. It is unclear how such a thick ductile zone could be generating tremor. Audet and Schaeffer (2018) also note that the LVZ does not extend into the locked zone; and on the down-dip side, it truncates at the mantle wedge. They conclude that the nature of the LVZ remains ambiguous and provide a couple of hypothesis explaining the increasing thickness of the LVZ with depth. These hypothesis, however, do not provide a definitive explanation of the periodic nature of slow slip.

2.3 Tremor

Since the first reporting by Obara (2002), tremor in subduction zones has been widely observed all over the world. Several researchers have reported that tremor has a dominant thrust-type focal mechanism (Shelly et al., 2006; Wech & Creager, 2007; Ide et al., 2007; Bostock et al., 2012), thereby providing a significant boost to the proponents of the Slow-Slip hypothesis. As the subducting slab slides underneath the continental crust during slow slip, it generates tremor with predominant thrust-type focal mechanism.

Tectonic tremors are usually located in a narrow spatial interval oriented in a strike-parallel direction (Wech et al., 2009; Kao et al., 2009; Obara et al., 2010; Audet et al., 2010; Audet & Schaeffer, 2018). The down-dip boundary is close to the mantle wedge, while the up-dip boundary extends a few kilometers from the mantle wedge. In the light of the Slow-Slip model, multiple explanations of their depth extent have been proposed, all of them revolving around variations in slip properties of the plate boundary due to temperature and pressure changes.

Multiple studies (Peterson & Christensen, 2009; Audet & Schaeffer, 2018) image the tremor swath to the down-dip side of the LVZ. Audet and Schaeffer (2018) interpret these observations as reflective of transitions in plate coupling and slip modes along the dip. If such transitions are indeed present, the processes that result in such changes along the plate boundary are open to question.

Tremors exhibit peculiar migration characteristics. Wech et al. (2009); Obara et al. (2011) observe up-dip and radial tremor migration. Obara et al. (2010, 2012) show a bimodal distribution of tremors in the Nankai subduction zone, with tremors from the along-strike migration concentrated on the up-dip side, while tremors from up-dip migration distributed over the entire tremor zone. Other studies (Houston et al., 2011; Obara et al., 2012) report rapid reverse tremor migration where tremors migrate in the opposite direction of along-strike migration at much faster speeds. It is unclear from the Slow-Slip hypothesis as to what physical phenomena might result in such migration patterns.

Schwartz and Rokosky (2007) find no evidence of slow slip and tremors in northeast Japan which has a thick old crust, while younger and thinner crusts in the Nankai subduction zone exhibit an array of slow slip events with varying periodicity. Wallace and Beavan (2010) report an interesting correlation between temporal characteristics of slow slip events and their depth of occurrence in the Hikurangi subduction margin of New Zealand. They note that the longest duration, and largest slow slip events occur at large depths, while the shortest duration, smallest, and most frequent slow slip events are usually shallow. Although the degree of plate coupling (Wallace & Beavan, 2010) can explain some of these observations, it is unclear how plate coupling can explain the variable periodicity and duration of the slow slip events.

2.4 Crustal Seismicity

Significant crustal seismicity is observed in Cascadia (Nicholson et al., 2005; Kao et al., 2005; Bostock et al., 2012) and Nankai (Shelly et al., 2006) subduction zones. A majority of the reported crustal seismicity is located at shallow depths and a few kilometer above the tremor zone and further landward. The Slow-Slip hypothesis does not provide a satisfactory explanation either of the origin of such seismicity or for the spatial correspondence between shallow crustal seismicity and deep tremor.

2.5 Mantle Helium

Sano et al. (2014) report interesting findings and suggest the existence of fluid pathways from the mantle to the trench in the Nankai subduction zone. They note, "a sharp increase in mantle-derived helium in bottom seawater near the rupture zone 1 month after the earthquake. The timing and location indicate that fluids were released from the mantle on the seafloor along the plate interface. The movement of the fluids was rapid, with a velocity of $\approx$4km per day and an uncertainty factor of four. This rate is much faster than what would be expected from pressure-gradient propagation, suggesting that over-pressurized fluid is discharged along the plate interface." It is debatable as to what forces mantle fluids to squirt out in the vicinity of the rupture zone during megathrust earthquakes.

Furthermore, Umeda et al. (2007) observe a close spatial correspondence between mantle helium and tremors. They report a high flux of mantle helium over regions experiencing tremors and a low flux in areas adjacent to those lacking tremors. Reconciling these observations with slow slip had proved to be challenging.

2.6 Paleo-Uplift and Subsidence

Evidence of large-scale and periodic continental deformation can be found in geologic records. Sherrod (2001) find evidence of abrupt sea level changes and rapid submergence in Puget Sound, Washington State. They estimate a maximum subsidence of approximately 3 m. Leonard et al. (2004) report a maximum subsidence of 2 m during the 1700 great Cascadia earthquake. In Alaska, Hamilton and Shennan (2005); Hamilton et al. (2005); Shennan and Hamilton (2006) report rapid subsidence measuring 2 m. It is unclear from the Slow-Slip model as to how the crust can experience an uplift in excess of 2 m over a period of 500 years.

3 Episodic Buckling and Collapse

The Slow-Slip hypothesis depicts a plate interface that is frictionally locked at shallow depths and transitions into a slow-slip zone down-dip. Below this transition zone, geoscientists believe that the subducting slab slides continuously at a steady rate consistent with plate motion. The key assumption in these models is that the overriding continental plate is in physical contact with the subducting oceanic slab all along the plate interface.

The Episodic Buckling and Collapse model, on the other hand, is based on the hypothesis of a buckling overriding plate that detaches itself down-dip from the subducting slab, while being in contact in the locked seismogenic zone. According to this model, the observed low-velocity zone (LVZ) is neither a part of the continental crust nor the subducting slab. Instead, it is a fluid-filled cavity created between the two plates because of the buckling of the overriding continental plate. An interplay of plate deformation, pressure differentials, and pressure release control the fluid flow in and out of this cavity and also generate seismicity in the form of tectonic tremor, low-frequency and very-low-frequency energy releases.

3.1 Euler Buckling

Under compressive stresses slender beams spontaneously bend to form curved shapes (Timoshenko & Gere, 1961). In subduction zones, the overriding continental crust acts as a collection of parallel slender beams (because of the plane stress imposed by the subducting slab) and buckles under the immense compressive stress applied by the subducting slab. A schematic scenario of buckling experienced by the continental crust is shown in Figure 1. The seaward locked zone and the landward thick continental crust result in an Euler buckling mode where both ends are fixed (Timoshenko & Gere, 1961). The seaward end, however, can slide because of the landward movement of the oceanic crust (Figure 1). Such a buckling mode results in not only horizontal displacements but also significant vertical strain in the continental crust.

Note that the short-term buckling and collapse cycles described below are sequences that make up each long-term megathrust cycle. Therefore, each megathrust cycle can be considered to be one centuries-long buckling and collapse cycle which in turn is made up of numerous short-term cycles. Dragert et al. (1994); Sherrod (2001); Leonard et al. (2004); Hamilton and Shennan (2005); Hamilton et al. (2005); Shennan and Hamilton (2006) present evidence of such long-term buckling and collapse cycles. At the start of the megathrust buckling cycle, the continential crust is in direct contact with the subducting slab at all depths. However, with each short-term buckling cycle, there is a net positive accumulation of strain within the continental crust, and progressive vertical detachment of the crust and slab as depicted below.

Below, we describe the various temporal phases of the short-term buckling process within each cycle and the multiple physical phenomena occurring within each of the phases.

3.2 Phase T_0

Because only the seaward edge of the plate interface (accretionary wedge and seismogenic zone) is 'locked' while the rest of the interface can slide, the overriding plate will buckle under the forces of the subduction process. Given the slowly developing subduction processes, the system will exhibit Euler's fundamental model of buckling – with the locked portion of the continental plate acting as one fixed end and the thick continental crust further inland serving as the other fixed end of the buckling system. Figure 2 shows a schematic of the buckling and collapse process occurring in subduction zones. Phase T_0 corresponds to a state within the buckling cycle where the tectonic stresses

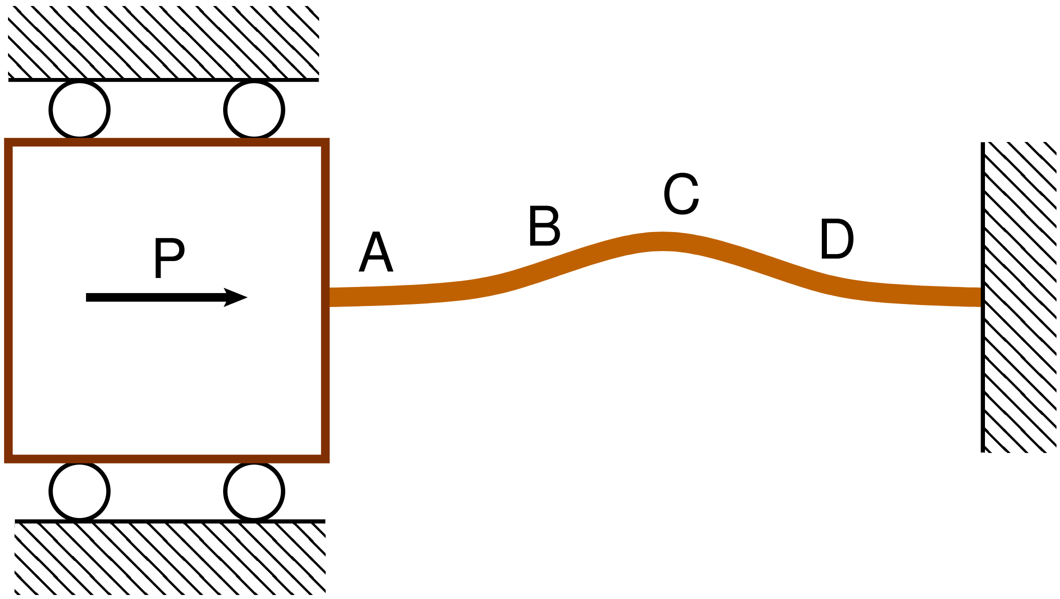

Figure 1: **Schematic of Euler buckling mode with both ends fixed.** Stress P is applied by the subducting slab at the locked zone (seaward fixed end). The landward fixed end results from the immoveable backarc continental crust. Locations A, B, C, and D, correspond to the positions on the continental crust shown in Figure 2 with their net displacement analyzed in Figure A1.

on the overriding continental plate are minimal (phase T_0, Figure 2). A magmatic-fluid-filled cavity exists between the overriding plate and the subducting slab.

3.3 Phase T_1

As the oceanic slab subducts, compressive stresses build up within the overriding plate, thereby pushing it upward and landward (phase T_1, Figure 2). The overriding plate starts buckling further to accommodate the additional strain, wherein the deep continental crust overlying the transition zone and the mantle wedge buckles away from the subducting slab and possibly the mantle.

3.3.1 Fluid Flow

The above deformation enlarges the size of the fluid-filled cavity and drives down the pore-pressure inside it, which in turn results in upwelling of magmatic fluids from the wedge region towards the cavity (Figure 3a). This process is slow and occurs for majority of the cycle. For example, in Cascadia, phase T_1 continues for majority of the 14 months. Because this phase evolves slowly, pressure equilibrium is maintained throughout the phase as progressive buckling is accompanied by steady fluid upwelling.

3.3.2 Low Effective Stress

We expect the effective stress of the system to be close to zero and any small stress perturbations may lead to escape of fluids through faults, fractures, fissures (and potentially magma vents), and also result in minor collapse of the overriding plate thereby generating tremor. Evidence of low effective normal stress comes from observations that tremors may not only be triggered by earthquakes (Brodsky & Mori, 2007; Miyazawa et al., 2008;

Rubinstein et al., 2007; Peng & Chao, 2008) but also, more interestingly, by tides (Shelly et al., 2007; Rubinstein et al., 2008; Hawthorne & Rubin, 2010).

Surface bulging due to buckling is consistent with the tiltmeter measurements (phases T_2, T_3, and T_4, Figure 2) as reported by Hirose and Obara (2005); Obara et al. (2004) who observe that the surface is dome shaped during tremor episodes. It would be interesting to study and quantify the temporal evolution in spatial patterns of tiltmeter measurements.

3.4 Phase T_2

Progressive buckling will result in continual opening of faults and fractures, with the openings starting at shallow depths and progressing downwards. At a certain critical state, right before the fracture and fault openings reach the fluid-filled cavity, buckling exhibits the maximal horizontal and vertical displacements of the overriding plate (phase T_2, Figure 2) within each cycle.

Phase T_2 also corresponds to the maximal extensional stress on the top of the overriding plate and the maximal volume of the fluid cavity within each cycle. The structure of the fluid cavity would be similar to what has been observed by Hansen et al. (2012); Toya et al. (2017); Audet and Schaeffer (2018) – thickening of the LVZ with increasing depth. Our model suggests that the LVZ extends into the continental Moho and truncates to the landward-side of the mantle wedge. The weak continental Moho reflectivity observed in the Cascadia subduction zone by Haney et al. (2016) is evidence of the LVZ extending landward into the continental Moho. Detailed imaging studies are needed to establish the precise landward-extent of this fluid cavity.

The time between Phases T_0 and T_2 corresponds to gradual buckling and slow upwelling of fluids. Such gradual deformations and steady fluid flow do not emanate any seismic energy in the vicinity of the plate boundary. However, the continual buckling and bulging of the overriding continental plate result in opening of strike-parallel and transverse faults resulting in significant crustal seismicity as observed by Nicholson et al. (2005); Shelly et al. (2006); Bostock et al. (2012). The shallow crust is expected to house a majority of this seismicity because it experiences the maximum strain.

3.5 Phase T_3

3.5.1 Fluid Cavity Collapse

As soon as the fault and fracture openings reach the fluid-filled cavity, the magmatic fluid escapes into the overriding plate (most likely accompanied by phase change from liquid to gaseous) and consequently drops the pressure inside the cavity dramatically (Figure 3b).

As a result, the cavity starts collapsing as illustrated in phase T_3 of Figure 2. The rapid reversal observed in horizontal GPS measurements is a result of the collapse-related seaward horizontal displacement and not from so-called slow slip. As shown below and as expected, changes in vertical displacement are even more substantial.

Wells et al. (2017) demonstrate substantial evidence of regional faults extending to the plate interface. The distribution of mantle helium in eastern Kyushu by Umeda et al. (2007) is consistent with the above picture. Umeda et al. (2007) observe a close correspondence of mantle helium (in hot springs) with the occurrence of tremor – the flux of mantle helium is low in areas lacking tremors, while it is high above regions experiencing tremors.

3.5.2 Fluid Flow

The rapid collapse of the continental plate will dramatically increase the fluid pressure inside the cavity, which in turn will push the fluid up-dip, down-dip, and along-strike (phases T_3, and T_4, Figures 2 and 3).

Also, there is a distinct possibility that the high fluid pressure fluids breaks flow barriers within conduits and asperities housed in the locked zone and the accretionary prism, leading to the up-dip escape of some magmatic fluids along the locked zone through the accretionary prism (Figure 3b). The collapsing continental plate will also push fluids along-strike at the plate boundary as shown below in phase T_4.

3.5.3 VLFEs

We hypothesize that the so-called shallow very-low-frequency earthquakes (VLFEs) observed in accretionary prisms result from the rapid flow of magmatic-fluid brought about by the collapsing continental crust.

Multiple researchers have reported the close spatial and temporal correspondence of shallow very-low-frequency earthquakes (VLFEs) in the accretionary prism with deep tremor and short-term slow slip events. Obara and Ito (2005) report shallow VLFEs on the up-dip side of the locked zone in the Nankai trough. Because the accretionary prism contains out-of-sequence thrusts and fault splays, Obara and Ito (2005) speculate that these fault planes might provide pathways for fluid flow from the subducting slab. More recently, the work of Liu et al. (2015); Nakano et al. (2018) shows the close temporal association between shallow VLFEs in the accretionary prism with deep short-term slow slip events. Liu et al. (2015) provide clear evidence of the occurrence of VLFEs predominantly at the onset of short-term slow slip. They also show that these VLFEs have thrust-type focal mechanism.

We do not expect any seismicity at the plate boundary (due to plate motion or fluid flow) during the buckling phase (phases T_0, and T_1, Figure 2) but expect different forms of energy release (at multiple locations on the plate boundary) during the collapse phases (phases T_3, and T_4, Figure 2) arising from plate striking as well as fluid flow.

3.5.4 Other Explanations for Cavity Collapse

The locked zone experiences substantial stress because of the buckling continental plate. Another possible scenario for the overriding plate collapse could be the minor and temporary decoupling of the locked zone when frictional forces in the locked zone are exceeded. Focal mechanisms of such seismic activity should be close to thrust-type. However, the lack of significant conventional seismicity (high frequency) in the locked zone prior to tremors is a strike against this possibility. Any future discovery of locked-zone conventional seismicity immediately preceding tremor activity will add substantial credibility to this potential scenario.

It is also possible that a combination of the above two processes – fluid flow and locked-zone decoupling, might be occurring. Future research efforts on understanding the dynamic processes at locked zone and the accretionary prism will shed more light on the dominant mechanism.

3.6 Phase T_4

3.6.1 Tectonic Tremor Origin

The rapidly collapsing overriding plate strikes the subducting oceanic slab, thereby generating tectonic tremor (phase T_4 of Figure 2). Tremor source mechanisms at subduction zones should therefore be dominantly of the Compensated Linear Vector Dipole (CLVD) type, with a possible minor thrusting component arising from the relative plate motion. Researchers have, however, observed a dominant thrust-type focal mechanism for tremor (Shelly et al., 2006; Wech & Creager, 2007; Ide et al., 2007; Bostock et al., 2012). That said, there is considerable similarity between the focal mechanisms of thrusting-type and of CLVD-type. In the absence of full-azimuth and wide-angle sampling of a focal sphere, one might mistake a CLVD mechanism as a thrust-type mechanism (especially if one is looking for it).

The atypical lower-boundary geometry of the buckled continental plate explains why tremors truncate at the continental Moho (phase T_4, Figure 2) and are observed lying within a narrow band up-dip along the plate interface (phase T_4, Figure 2, Wech et al., 2009; Peterson & Christensen, 2009; Audet & Schaeffer, 2018). Audet et al. (2010) note that "the peak occurrence of tremors roughly coincides with the intersection of the plate interface with the overlying continental crust–mantle boundary". In addition, as supporting frictional forces are overcome, the lower portion of the continental crust wedge strikes the subducting slab first (phase T_4, Figure 2), followed by a progressive collapse of the continental crust along the up-dip (and radial) direction (phase T_4, Figure 3c) – interpreted as up-dip and radial tremor migration in several studies (Wech et al., 2009; Obara et al., 2011).

3.6.2 Fluid Flow

As the overriding continental crust collapses with the lower edge hitting the subducting slab first, some of the fluids are pushed landward along the continental Moho, while most of the fluids are pushed up-dip and along-strike (Figure 3c). It is likely that as the lower edge hits the subducting slab, it cuts off hydraulic communication between the up-dip fluid cavity and the down-dip mantle wedge, thereby trapping fluid in the cavity. As described above, the collapse also increases the pore-pressure in the cavity, without which the up-dip rate of collapse (parameter that controls tremor migration rate) would be larger than the ones observed by Wech et al. (2009) and Obara et al. (2011) in Cascadia and Japan, respectively. In the latter part of phase T_4, the lagging end of the high-pressure fluid pocket collapses (creating tremors), thereby pushing the fluid pocket up-dip and parallel to the strike along the plate boundary.

Similar to shallow VLFEs, we hypothesize that deep low-frequency earthquakes (LFEs and VLFEs), observed by many researchers (e.g. Ito et al., 2007, 2009; Matsuzawa et al., 2009; Obara, 2011), correspond to the rapid sloshing of magmatic fluids brought about by the hastened collapse of the overriding plate. The up-dip location of deep VLFEs with respect to that of tremor indicates that most of the magmatic fluid is pushed up-dip in phases 3 and 4 (Figure 3b and 3c).

The periodic changes in seismicity rates and attenuation and their correspondence with accelerated slow slip, as reported by Nakajima and Uchida (2018), corroborates the above model of fluid flow in and out of the fluid cavity. The 'breathing' mechanism of magmatic fluid flow driven by periodic plate deformation in subduction zones might be the dominant mechanism (and not buoyancy) of magma transport from the upper mantle to the crust and might even be responsible for the creation of the Aleutian Volcanic Arc in Alaska and its volcanism as evident from the focusing of partial melt under the arc.

3.6.3 Tremor Migration

The locked zone prevents the fluid pocket from moving further up-dip and therefore the fluid pocket migrates parallel to the margin and down-dip of the locked zone as depicted in Figure 3c. In the latter part of phase T_4, we believe that the trapped fluids move predominantly along-strike until fluids are lost to the overlying permeable crust. For the fluids to migrate along-strike, the plates need to detach from each other. We posit that the detachment process results in the observed along-strike tremor migration (Wech et al., 2009; Obara et al., 2011, 2012). Because of the low fluid-pressure in the latter stages, the rate of detachment is expected to be lower than the initial up-dip collapse rate – which explains the slower along-strike tremor migration with respect to up-dip migration (Wech et al., 2009; Houston et al., 2011; Obara et al., 2011, 2012). This model also explains the bimodal distribution of tremors in the Nankai subduction zone (Obara et al., 2012) with tremors from the along-strike migration concentrated on the up-dip side while tremors from up-dip migration are distributed over the entire tremor zone.

Some studies (Houston et al., 2011; Obara et al., 2012) also report rapid reverse tremor migration where tremors migrate in the opposite direction of along-strike migration at much faster speeds. We postulate that rapid tremor reversal happens when a migrating high-pressure fluid pocket encounters a permeable zone such as a fault or fracture zone, or a magma vent or dike (Figure 3c). As fluid escapes through these fissures, the leading edge of the fluid pocket collapses rapidly. This collapse is in the direction opposite to the migrating fluid front and occurs at a much faster rate given the loss of pore pressure in the fluid pocket.

Note that the fluid cavity does not fully collapse within each cycle, instead there is a partial collapse. However, with each passing cycle we expect the size of the fluid cavity to increase. Only when the frictional forces in the locked zone are overcome during the megathrust earthquake, does the fluid cavity completely collapse.

Note that tremors and so-called slow slip events display a wide range of periodicity in the Nankai and Hikurangi subduction zones (Schwartz & Rokosky, 2007; Wallace & Beavan, 2010; Obara, 2011) – with the seismicity characteristics clearly correlated to the depth of the seismicity (Wallace & Beavan, 2010). The Episodic Buckling and Collapse model provides a reasonable explanation for these observations. A thinner crust is more easily buckled than a thicker one; at the same time, the thinner crust can accommodate a lesser degree of strain energy than a thicker one. Hence, a thinner crust will undergo more cycles of episodic buckling and collapse than a thicker one within the same time period, all the while releasing lesser seismic energy in each cycle.

4 Discussion

Although majority of the strain in the overriding plate is released when it collapses, a small portion of the strain is retained in every cycle. Over hundreds of buckling and collapse cycles, the small retained strains add up and this strain energy is stored in the overriding continental plate. A critical state is attained where the forces exerted by the stored elastic energy (due to compression) and gravitational potential energy (stored in the uplifted continental crust) equates the frictional forces in the seismogenic zone. This state of deformation exhibits the maximal horizontal and vertical displacements of the overriding plate. When the frictional forces are exceeded, the stored energy is released in the form of a megathrust earthquake. Evidence of these inter-seismic crustal deformations corresponding to megathrust earthquakes is found in long-term geologic records (Dragert et al., 1994; Sherrod, 2001; Leonard et al., 2004; Hamilton & Shennan, 2005; Hamilton et al., 2005; Shennan & Hamilton, 2006) and may be interpreted as large time-scale versions of the buckling process that take centuries to develop. The rapid subsidence, observed by Sherrod (2001); Leonard et al. (2004); Hamilton and Shennan (2005); Hamilton et al. (2005); Shennan and Hamilton (2006) on geologic records, occurs during the express subsidence of the overriding continental plate.

As the continental plate completely collapses after a megathrust earthquake, the horizontal component of the GPS shows large seaward displacements and the vertical

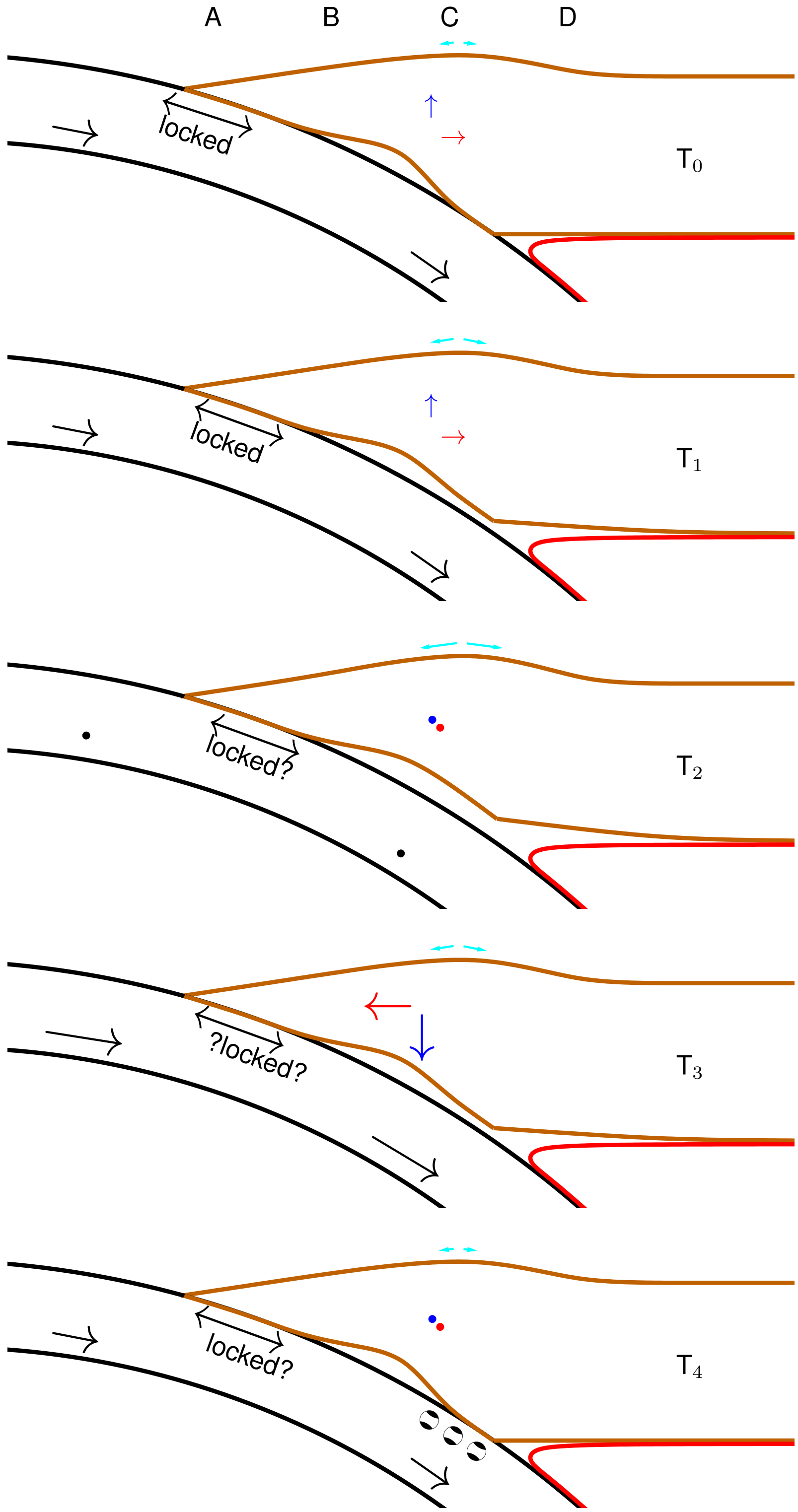

Figure 2: **Schematic illustration of the different phases of the Episodic Buckling and Collapse model of the subduction process and the structural changes therein.** The subducting oceanic crust is outlined by black lines and the black arrows represent the direction and magnitude of the slab velocity. The overriding continental crust is represented by the solid brown lines. Red and blue arrows represent the magnitudes of the instantaneous horizontal and vertical velocities, respectively, of a point in the continental crust wedge. Dots in Phases T_0, T_2, and T_4 represent vectors of magnitude zero. The tilt magnitude and direction are denoted by the arrows in cyan. The side-view of CLVD focal spheres are shown along the plate interface. Temporal motion of locations A through D on the continental crust surface are analyzed in Figure A1 below.

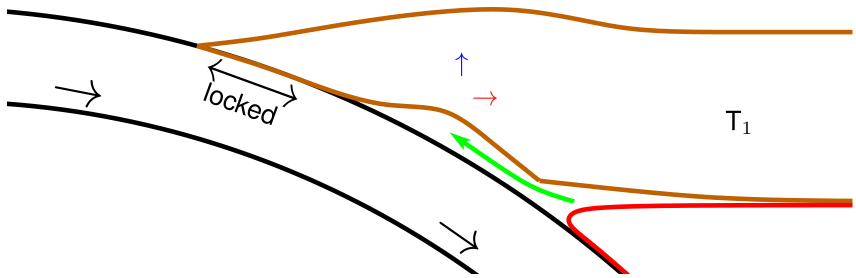

(a) Phase T_1

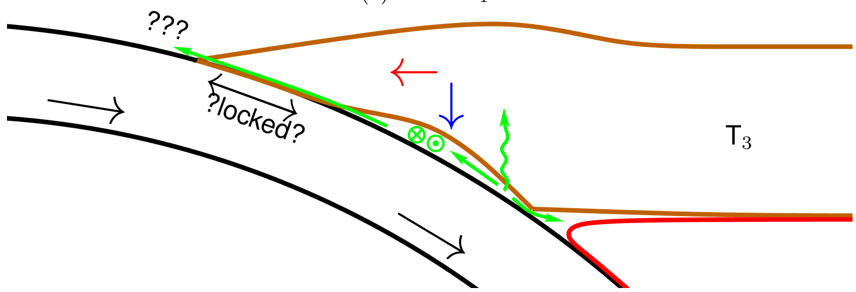

(b) Phase T_3

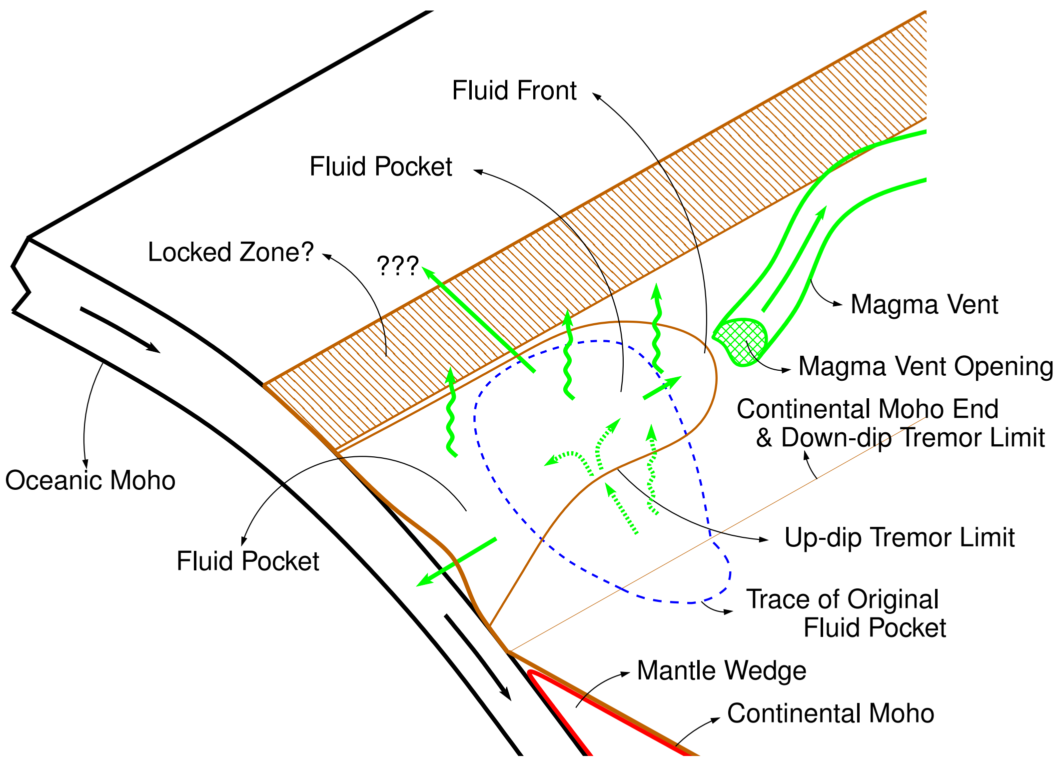

(c) Phase T_4

Figure 3: **Schematic illustration of magmatic fluid flow during each Episodic Buckling and Collapse cycle. a,b,** Two-dimensional crosssections for phases T_1 and T_3 are shown while **c,** phase T_4 is shown in three-dimensions. In **c,** only the basal surface of the continental crust is shown for clarity. The subducting oceanic crust is outlined by black lines and the black arrows represent the direction and magnitude of the slab velocity. The overriding continental crust is represented by the solid brown lines and the mantle is demarcated by the thick red line. Green arrows represent the flow direction of magmatic fluids. Boundary of the original cavity generated during buckling is marked by the dashed blue line.

component shows significant subsidence. The large "aseismic afterslip", following megathrust earthquakes and observed in multiple studies (J. S. Gomberg et al., 2012; Rolandone et al., 2018), is simply the horizontal projection of the seaward surface displacement of the overriding continental plate. Also, because the overriding plate gradually collapses while pushing fluids out (instead of sliding on the oceanic slab), there is no seismic energy released – it is aseismic. The magmatic fluids are most likely pushed out along-strike and to the trench along the ruptured plate boundary as evidenced by the significant increase in mantle helium in the seawater and reported by Sano et al. (2014).

As suspected by several geoscientists, the periodic release of stored energy in subduction zones in the form of fluid flow and seismic events, during each Episodic Buckling and Collapse cycle, indeed prevents megathrust earthquakes from occurring more frequently. A back-of-the-envelope calculation shows that if not for the episodic energy release, the Cascadia region would be experiencing one megathrust earthquakes every 54 years.

Therefore, we believe that the key to forecasting megathrust earthquakes in a cost-effective fashion is to monitor long-term trends (in the order of decades and centuries) in ground deformation through multi-component GPS and tiltmeter recordings. In addition, use of a dynamic modulus of continental crust in numerical simulation of deformation will also help improve megathrust forecasting.

Acknowledgments

Partial funding for is provided by the National Science Foundation under the EAGER program (NSF Grant 1933169). In Cascadia, GPS time series are provided by the Pacific Northwest Geodetic Array, Central Washington University (https://www.geodesy.cwu.edu/). For Alaska, GPS time series data were downloaded from USGS (https://earthquake.usgs.gov/monitoring/gps). We thank Manika Prasad for discussions.

References

Audet, P., Bostock, M. G., Boyarko, D. C., Brudzinski, M. R., & Allen, R. M. (2010, feb). Slab morphology in the Cascadia fore arc and its relation to episodic tremor and slip. *Journal of Geophysical Research*, *115*. doi: 10.1029/2008jb006053

Audet, P., Bostock, M. G., Christensen, N. I., & Peacock, S. M. (2009). Seismic evidence for overpressured subducted oceanic crust and megathrust fault sealing. *Nature*, *457*(7225), 76–78. doi: 10.1038/nature07650

Audet, P., & Schaeffer, A. J. (2018). Fluid pressure and shear zone development over the locked to slow slip region in Cascadia. *Science Advances*, *4*(3). doi: 10.1126/sciadv.aar2982

Behura, J., Prasad, M., & Forghani, F. (2018, dec). Episodic Buckling and Collapse - The Breathing Subduction Zones. In *AGU Fall Meeting Abstracts* (Vol. 2018, pp. T21F–0289).

Bell, R., Sutherland, R., Barker, D. H. N., Henrys, S., Bannister, S., Wallace, L., & Beavan, J. (2010). Seismic reflection character of the Hikurangi subduction interface, New Zealand, in the region of repeated Gisborne slow slip events. *Geophysical Journal International*, *180*(1), 34–48. doi: 10.1111/j.1365-246x.2009.04401.x

Beroza, G. C., & Ide, S. (2011). Slow Earthquakes and Nonvolcanic Tremor. *Annual Review of Earth and Planetary Sciences*, *39*(1), 271–296. doi: 10.1146/annurev-earth-040809-152531

Bettinelli, P., Avouac, J.-P., Flouzat, M., Bollinger, L., Ramillien, G., Rajaure, S., & Sapkota, S. (2008). Seasonal variations of seismicity and geodetic strain in the Himalaya induced by surface hydrology. *Earth and Planetary Science Letters*, *266*(3), 332–344. Retrieved from http://www.sciencedirect.com/science/article/pii/S0012821X07007492 doi: 10.1016/j.epsl.2007.11.021

Blewitt, G., Lavallée, D., Clarke, P., & Nurutdinov, K. (2001). A New Global Mode of Earth Deformation: Seasonal Cycle Detected. *Science*, *294*(5550), 2342–2345. Retrieved from https://science.sciencemag.org/content/294/5550/2342 doi: 10.1126/science.1065328

Bostock, M. G., Royer, A. A., Hearn, E. H., & Peacock, S. M. (2012). Low frequency earthquakes below southern Vancouver Island. *Geochemistry, Geophysics, Geosystems*, *13*(11), n/a—n/a. Retrieved from http://dx.doi.org/10.1029/2012GC004391 doi: 10.1029/2012GC004391

Boyarko, D. C., & Brudzinski, M. R. (2010). Spatial and temporal patterns of nonvolcanic tremor along the southern Cascadia subduction zone. *Journal of Geophysical Research*, *115*. doi: 10.1029/2008jb006064

Brodsky, E. E., & Mori, J. (2007). Creep events slip less than ordinary earthquakes. *Geophysical Research Letters*, *34*(16). doi: 10.1029/2007gl030917

Dong, D., Fang, P., Bock, Y., Cheng, M. K., & Miyazaki, S. (2002). Anatomy of apparent seasonal variations from GPS-derived site position time series. *Journal of Geophysical Research: Solid Earth*, *107*(B4), ETG 9–1–ETG 9–16. Retrieved from https://agupubs.onlinelibrary.wiley.com/doi/abs/10.1029/2001JB000573 doi: 10.1029/2001JB000573

Douglas, A. (2005). Slow slip on the northern Hikurangi subduction interface, New Zealand. *Geophysical Research Letters*, *32*(16). doi: 10.1029/2005gl023607

Dragert, H., Hyndman, R. D., Rogers, G. C., & Wang, K. (1994, oct). Current deformation and the width of the seismogenic zone of the northern Cascadia subduction thrust. *Journal of Geophysical Research: Solid Earth*, *99*(B1), 653–668. doi: 10.1029/93jb02516

Dragert, H., Wang, K., & James, T. S. (2001). A Silent Slip Event on the Deeper Cascadia Subduction Interface. *Science*. doi: 10.1126/science.1060152

Eberhart-Phillips, D., Christensen, D. H., Brocher, T. M., Hansen, R., Ruppert, N. A., Haeussler, P. J., & Abers, G. A. (2006). Imaging the transition from Aleutian subduction to Yakutat collision in central Alaska, with local earthquakes and active source data. *Journal of Geophysical Research: Solid Earth*, *111*(B11). doi: 10.1029/2005jb004240

Ghosh, A., Vidale, J. E., Sweet, J. R., Creager, K. C., Wech, A. G., Houston, H., & Brodsky, E. E. (2010). Rapid, continuous streaking of tremor in Cascadia. *Geochemistry, Geophysics, Geosystems*, *11*(12). doi: 10.1029/2010gc003305

Gomberg, J. (2010). Slow-slip phenomena in Cascadia from 2007 and beyond: A review. *Geological Society of America Bulletin*, *122*(7-8), 963–978. doi: 10.1130/b30287.1

Gomberg, J. S., Prejean, S. G., & Ruppert, N. A. (2012). Afterslip, Tremor, and the Denali Fault Earthquake..

Hamilton, S., & Shennan, I. (2005). Late Holocene relative sea-level changes and the earthquake deformation cycle around upper Cook Inlet, Alaska. *Quaternary Science Reviews*, *24*(12), 1479–1498. Retrieved from http://www.sciencedirect.com/science/article/pii/S0277379104003269 doi: 10.1016/j.quascirev.2004.11.003

Hamilton, S., Shennan, I., Combellick, R., Mulholland, J., & Noble, C. (2005). Evidence for two great earthquakes at Anchorage, Alaska and implications for multiple great earthquakes through the Holocene. *Quaternary Science Reviews*, *24*(18), 2050–2068. Retrieved from http://www.sciencedirect.com/science/article/pii/S0277379105001289 doi: 10.1016/j.quascirev.2004.07.027

Haney, M. M., Tsai, V. C., & Ward, K. M. (2016). Widespread imaging of the lower crust, Moho, and upper mantle from Rayleigh waves: A comparison of the Cascadia and Aleutian-Alaska subduction zones. *2015 Fall Meeting, AGU*.

Hansen, R., Bostock, M., & Christensen, N. (2012, jul). Nature of the low velocity zone in Cascadia from receiver function waveform inversion. *Earth and Planetary Science Letters*, *337*, 25–38. doi: 10.1016/j.epsl.2012.05.031

Hawthorne, J. C., & Rubin, A. M. (2010). Tidal modulation of slow slip in Cascadia. *Journal of Geophysical Research*, *115*(B9). doi: 10.1029/2010jb007502

Heki, K., & Kataoka, T. (2008, apr). On the biannually repeating slow-slip events at the Ryukyu Trench, southwestern Japan. *Journal of Geophysical Research*, *113*(B11). doi: 10.1029/2008jb005739

Hirose, H., Hirahara, K., Kimata, F., Fujii, N., & Miyazaki, S. (1999, jan). A slow thrust slip event following the two 1996 Hyuganada Earthquakes beneath the Bungo Channel, southwest Japan. *Geophysical Research Letters*, *26*(21), 3237–3240. doi: 10.1029/1999gl010999

Hirose, H., & Obara, K. (2005). Repeating short- and long-term slow slip events with deep tremor activity around the Bungo channel region, southwest Japan. *Earth, Planets and Space*, *57*(10), 961–972. doi: 10.1186/bf03351875

Hirose, H., & Obara, K. (2010). Recurrence behavior of short-term slow slip and correlated nonvolcanic tremor episodes in western Shikoku, southwest Japan. *Journal of Geophysical Research*, *115*. doi: 10.1029/2008jb006050

Houston, H., Delbridge, B. G., Wech, A. G., & Creager, K. C. (2011). Rapid tremor reversals in Cascadia generated by a weakened plate interface. *Nature Geoscience*, *4*(6), 404–409. doi: 10.1038/ngeo1157

Ide, S., Shelly, D. R., & Beroza, G. C. (2007). Mechanism of deep low frequency earthquakes: Further evidence that deep non-volcanic tremor is generated by shear slip on the plate interface. *Geophysical Research Letters*.

Ito, Y., Obara, K., Matsuzawa, T., & Maeda, T. (2009). *Very low frequency earthquakes related to small asperities on the plate boundary interface at the locked to aseismic transition* (Vol. 114) (No. B11). Retrieved from `https://agupubs.onlinelibrary.wiley.com/doi/abs/10.1029/2008JB006036` doi: 10.1029/2008JB006036

Ito, Y., Obara, K., Shiomi, K., Sekine, S., & Hirose, H. (2007). Slow Earthquakes Coincident with Episodic Tremors and Slow Slip Events. *Science*, *315*(5811), 503–506. doi: 10.1126/science.1134454

Kao, H., Shan, S.-J., Dragert, H., & Rogers, G. (2009). Northern Cascadia episodic tremor and slip: A decade of tremor observations from 1997 to 2007. *Journal of Geophysical Research: Solid Earth*, *114*(B11). doi: 10.1029/2008jb006046

Kao, H., Shan, S.-J., Dragert, H., Rogers, G., Cassidy, J. F., & Ramachandran, K. (2005). A wide depth distribution of seismic tremors along the northern Cascadia margin. *Nature*, *436*(7052), 841–844. doi: 10.1038/nature03903

Leonard, L. J., Hyndman, R. D., & Mazzotti, S. (2004). Coseismic subsidence in the 1700 great Cascadia earthquake: Coastal estimates versus elastic dislocation models. *Geological Society of America Bulletin*, *116*(5), 655. doi: 10.1130/b25369.1

Liu, Z., Moore, A. W., & Owen, S. (2015). Recurrent slow slip event reveals the interaction with seismic slow earthquakes and disruption from large earthquake. *Geophysical Journal International*, *202*(3), 1555–1565. Retrieved from `https://doi.org/10.1093/gji/ggv238` doi: 10.1093/gji/ggv238

Matsubara, M., Obara, K., & Kasahara, K. (2009). High-Vp/Vs zone accompanying non-volcanic tremors and slow-slip events beneath southwestern Japan. *Tectonophysics*, *472*(1-4), 6–17. doi: 10.1016/j.tecto.2008.06.013

Matsuzawa, T., Obara, K., & Maeda, T. (2009). Source duration of deep very low frequency earthquakes in western Shikoku, Japan. *Journal of Geophysical Research: Solid Earth*, *114*(B11). Retrieved from `https://agupubs.onlinelibrary.wiley.com/doi/abs/10.1029/2008JB006044` doi: 10.1029/2008JB006044

Miller, M. M., Melbourne, T., Johnson, D. J., & Sumner, W. Q. (2002, mar). Periodic slow earthquakes from the Cascadia subduction zone. *Science*, *295*(5564), 2423.

Miyazaki, S., Segall, P., Mcguire, J. J., Kato, T., & Hatanaka, Y. (2006). Spatial and temporal evolution of stress and slip rate during the 2000 Tokai slow earthquake. *Journal of Geophysical Research: Solid Earth*, *111*(B3). doi: 10.1029/2004jb003426

Miyazawa, M., Brodsky, E. E., & Mori, J. (2008). Learning from dynamic triggering of low-frequency tremor in subduction zones. *Earth, Planets and Space*, *60*(10). doi: 10.1186/bf03352858

Nakajima, J., & Uchida, N. (2018, apr). Repeated drainage from megathrusts during episodic slow slip. *Nature Geoscience*, *11*(5), 351–356. doi: 10.1038/s41561-018-0090-z

Nakano, M., Hori, T., Araki, E., Kodaira, S., & Ide, S. (2018). Shallow very-low-frequency earthquakes accompany slow slip events in the Nankai subduction zone. *Nature Communications*, *9*. doi: 10.1038/s41467-018-03431-5

Nicholson, T., Bostock, M., & Cassidy, J. F. (2005). New constraints on subduction zone structure in northern Cascadia. *Geophysical Journal International*, *161*(3), 849–859. Retrieved from `https://doi.org/10.1111/j.1365-246X.2005.02605.x` doi: 10.1111/j.1365-246X.2005.02605.x

Obara, K. (2002, may). Nonvolcanic deep tremor associated with subduction in southwest Japan. *Science*, *296*(5573), 1679–1681.

Obara, K. (2011). Characteristics and interactions between non-volcanic tremor and related slow earthquakes in the Nankai subduction zone, southwest Japan. *Journal of Geodynamics*, *52*(3-4), 229–248. doi: 10.1016/j.jog.2011.04.002

Obara, K., Hirose, H., Yamamizu, F., & Kasahara, K. (2004, mar). Episodic slow slip events accompanied by non-volcanic tremors in southwest Japan subduction zone. *Geophysical Research Letters*, *31*(23). doi: 10.1029/2004gl020848

Obara, K., & Ito, Y. (2005, apr). Very low frequency earthquakes excited by the 2004 off the Kii peninsula earthquakes: A dynamic deformation process in the large accretionary prism. *Earth, Planets and Space*, *57*(4), 321–326. Retrieved from `https://doi.org/10.1186/BF03352570` doi: 10.1186/BF03352570

Obara, K., Matsuzawa, T., Tanaka, S., Kimura, T., & Maeda, T. (2011, oct). Migration properties of non-volcanic tremor in Shikoku, southwest Japan. *Geophysical Research Letters*, *38*(9). doi: 10.1029/2011gl047110

Obara, K., Matsuzawa, T., Tanaka, S., & Maeda, T. (2012). Depth-dependent mode of tremor migration beneath Kii Peninsula, Nankai subduction zone. *Geophysical Research Letters*, *39*(10). doi: 10.1029/2012gl051420

Obara, K., Tanaka, S., Maeda, T., & Matsuzawa, T. (2010). Depth-dependent activity of non-volcanic tremor in southwest Japan. *Geophysical Research Letters*, *37*(13). doi: 10.1029/2010GL043679

Ohta, K., Ito, Y., Hino, R., Ohyanagi, S., Matsuzawa, T., Shiobara, H., & Shinohara, M. (2019). Tremor and Inferred Slow Slip Associated With Afterslip of the 2011 Tohoku Earthquake. *Geophysical Research Letters*, *46*(9), 4591–4598. Retrieved from `https://agupubs.onlinelibrary.wiley.com/doi/abs/10.1029/2019GL082468` doi: 10.1029/2019GL082468

Ohta, Y., Freymueller, J., Hreinsdottir, S., & Suito, H. (2006). A large slow slip event and the depth of the seismogenic zone in the south central Alaska subduction zone. *Earth and Planetary Science Letters*, *247*(1-2), 108–116. doi: 10.1016/j.epsl.2006.05.013

Peng, Z., & Chao, K. (2008). Non-volcanic tremor beneath the Central Range in Taiwan triggered by the 2001 Mw 7.8 Kunlun earthquake. *Geophysical Journal International*, *175*(2), 825–829. doi: 10.1111/j.1365-246X.2008.03886.x

Peterson, C. L., & Christensen, D. H. (2009, apr). Possible relationship between nonvolcanic tremor and the 1998–2001 slow slip event, south central Alaska. *Journal of Geophysical Research*, *114*(B6). doi: 10.1029/2008jb006096

Rogers, G., & Dragert, H. (2003). Episodic Tremor and Slip on the Cascadia Subduction Zone: The Chatter of Silent Slip. *Science*, *300*(5627), 1942–1943. doi: 10.1126/science.1084783

Rolandone, F., Nocquet, J.-M., Mothes, P. A., Jarrin, P., Vallée, M., Cubas, N., ... Font, Y. (2018). Areas prone to slow slip events impede earthquake rupture propagation and promote afterslip. *Science Advances*, *4*(1). Retrieved from `https://advances.sciencemag.org/content/4/1/eaao6596` doi: 10.1126/sciadv.aao6596

Rubinstein, J. L., La Rocca, M., Vidale, J. E., Creager, K. C., & Wech, A. G. (2008, jan). Tidal modulation of nonvolcanic tremor. *Science*, *319*(5860), 186–189.

Rubinstein, J. L., Vidale, J. E., Gomberg, J., Bodin, P., Creager, K. C., & Malone, S. D. (2007). Non-volcanic tremor driven by large transient shear stresses. *Nature*, *448*(7153), 579–582. doi: 10.1038/nature06017

Sano, Y., Hara, T., Takahata, N., Kawagucci, S., Honda, M., Nishio, Y., ... Hattori, K. (2014, jan). *Helium anomalies suggest a fluid pathway from mantle to trench during the 2011 Tohoku-Oki earthquake.* Nature Publishing Group. Retrieved from `https://www.nature.com/articles/ncomms4084`

Schwartz, S. Y., & Rokosky, J. M. (2007). Slow slip events and seismic tremor at circum-Pacific subduction zones. *Reviews of Geophysics*, *45*(3). doi: 10.1029/2006rg000208

Shelly, D. R., Beroza, G. C., & Ide, S. (2007). Non-volcanic tremor and low-frequency earthquake swarms. *Nature*, *446*(7133), 305–307. doi: 10.1038/nature05666

Shelly, D. R., Beroza, G. C., Ide, S., & Nakamula, S. (2006, jul). Low-frequency earthquakes in Shikoku, Japan, and their relationship to episodic tremor and slip. *Nature*, *442*(7099), 188–191.

Shennan, I., & Hamilton, S. (2006). Coseismic and pre-seismic subsidence associated with great earthquakes in Alaska. *Quaternary Science Reviews*, *25*(1-2), 1–8. doi: 10.1016/j.quascirev.2005.09.002

Sherrod, B. L. (2001, oct). Evidence for earthquake-induced subsidence about 1100 yr ago in coastal marshes of southern Puget Sound, Washington. *Geological Society of America Bulletin*, *113*(10), 1299–1311. doi: 10.1130/0016-7606(2001)113⟨1299:EFEISA⟩2.0.CO;2

Timoshenko, S. P., & Gere, J. M. (1961). *Theory of elastic stability* (2nd ed.). McGraw-Hill.

Toya, M., Kato, A., Maeda, T., Obara, K., Takeda, T., & Yamaoka, K. (2017, jun). Down-dip variations in a subducting low-velocity zone linked to episodic tremor and slip: a new constraint from ScSp waves. *Scientific Reports*, *7*(1). doi: 10.1038/s41598-017-03048-6

Umeda, K., McCrank, G. F., & Ninomiya, A. (2007). Helium isotopes as geochemical indicators of a serpentinized fore-arc mantle wedge. *Journal of Geophysical Research: Solid Earth*, *112*(B10). Retrieved from `https://agupubs.onlinelibrary.wiley.com/doi/abs/10.1029/2007JB005031` doi: 10.1029/2007JB005031

Vidale, J. E., & Houston, H. (2012, jan). Slow slip: A new kind of earthquake. *Physics Today*, *65*(1), 38–43. doi: 10.1063/pt.3.1399

Wallace, L. M., & Beavan, J. (2010, feb). Diverse slow slip behavior at the Hikurangi subduction margin, New Zealand. *Journal of Geophysical Research*, *115*(B12). doi: 10.1029/2010jb007717

Wech, A. G., & Creager, K. C. (2007). Cascadia tremor polarization evidence for plate interface slip. *Geophysical Research Letters*, *34*(22). doi: 10.1029/2007gl031167

Wech, A. G., Creager, K. C., & Melbourne, T. I. (2009). Seismic and geodetic constraints on Cascadia slow slip. *Journal of Geophysical Research: Solid Earth*, *114*(B10). doi: 10.1029/2008JB006090

Wells, R. E., Blakely, R. J., Wech, A. G., McCrory, P. A., & Michael, A. (2017). Cascadia subduction tremor muted by crustal faults. *Geology*, *45*(6), 515–518. Retrieved from https://doi.org/10.1130/G38835.1 doi: 10.1130/G38835.1

Appendix A GPS Analysis

The hypothesis of episodic slow slip has been postulated by employing solely horizontal GPS recordings. Here, we use all three components of GPS recording (two horizontal and one vertical) to demonstrate the 3D deformation of the continental crust over time and how their magnitudes relate to tremor location.

A1 Reliability of Vertical GPS Measurements

Uncertainty in vertical GPS measurements is approximately 3 times that of horizontal measurements. More importantly, we recognize that seasonal variations in surface mass variations can have substantial impact on vertical GPS measurements Blewitt et al. (2001); Dong et al. (2002); Bettinelli et al. (2008).

Here, however, we ignore the effect of seasonal changes on vertical GPS measurements because it is extremely challenging to decouple the effect of seasonal surficial mass changes from displacement due to tectonic deformation. This task become especially challenging in Cascadia where the episodic deformation cycle spans 13–14 months which is close to seasonal cycles (12 months).

Nonetheless, we observe that

- vertical GPS measurements are large and in many cases an order of magnitude larger than horizontal displacements,
- there is a close correspondence between sudden changes in horizontal displacements (horizontal GPS reversals) and rapid vertical GPS measurements on numerous occasions, and
- vertical cyclic displacement patterns (Figure A3 and A4) show close spatial correspondence with spatial tremor patterns in Cascadia and Alaska.

Given the above observations, one might argue that vertical displacements observed contain significant imprints of tectonic deformation.

A2 Data Processing

Prior to hodogram analysis, GPS data are detrended using a 1001 point median filter to eliminate long-term trends, and thereafter filtered using a 11-point median filter to suppress short-term noise bursts. GPS stations with significant noise that could not be corrected from using the above filtering operations were not used in the analysis.

Computation of the net vertical and horizontal GPS displacements was done by fitting ellipsoids to the hodograms. Projection of the major axis of the ellipse on the vertical direction and the horizontal plane yield the net vertical and horizontal displacements, respectively.

A3 Displacements due to Buckling and Collapse

Figure A1 shows the expected temporal evolution of the vertical (blue) and horizontal (red) displacements of four locations A, B, C, and D, (phase T_0, Figure 2) on the surface of a continental plate through a buckling and collapsing cycle. The magnitude of the horizontal displacement is expected to decrease monotonically from the corner of the accretionary wedge (location A) landward as depicted by the decreasing range of the horizontal displacement moving from A through D. The vertical displacement, however, is small at location A, attains a maximum at location C, and tapers off to a small value further landwards (location D).

An efficient technique to analyze and quantify such multi-component data is to generate hodograms which are a display of the motion of a point as a function of time. Figure A1 shows the hodograms for each of the four locations A, B, C, and D on the right. The path followed by a particle during the buckling phase is different from that followed during the collapse phase, thereby resulting in hysteresis of the particle motion. Note that such hysteresis demonstrates a non-linear particle motion (Figure A1) as opposed to an expected linear motion for the case of slow slip. Moreover, it is clear from the hodograms that the horizontal displacement decreases monotonically from the corner of the accretionary wedge (location A) landward, while the vertical displacement attains a maximum right above the narrow tremor zone.

Figure A2 shows an example of a hodogram obtained from GPS data. This data comes from the Albert Head GPS site on Vancouver Island in Victoria, British Columbia – the data for which was originally employed by Rogers and Dragert (2003) to hypothesize the process of slow slip. Note the hysteresis and the prominent vertical displacement observed at this site which is quite similar to the pattern expected for surface location C (Figure A1) right above a tremor belt. Other studies (Wech et al., 2009; Wells et al., 2017) indeed map significant tremor activity beneath this GPS site.

A4 Horizontal and Vertical Displacements in Cascadia and Alaska

We generate hodograms for all the GPS measurements at sites in the Cascadia subduction zone and in Alaska and thereafter compute the vertical displacement, horizontal displacement, and their ratio. These attributes for Cascadia and Alaska are shown in Figures A3 and A4, respectively. Note that in both cases, the horizontal displacement decreases monotonically from the margin landwards; while the vertical displacement increases as one moves landwards from the margin, attains a maximum, and decreases thereafter. The belt of maximum vertical displacements along the Cascadia margin has a close correspondence to the tremor maps generated by Wech et al. (2009); Wells et al. (2017). Similarly, the maximum vertical displacements in Alaska encompass the tremor activity mapped by Y. Ohta et al. (2006) and Peterson and Christensen (2009) (in addition to showing locations where additional tremor activity could be expected).

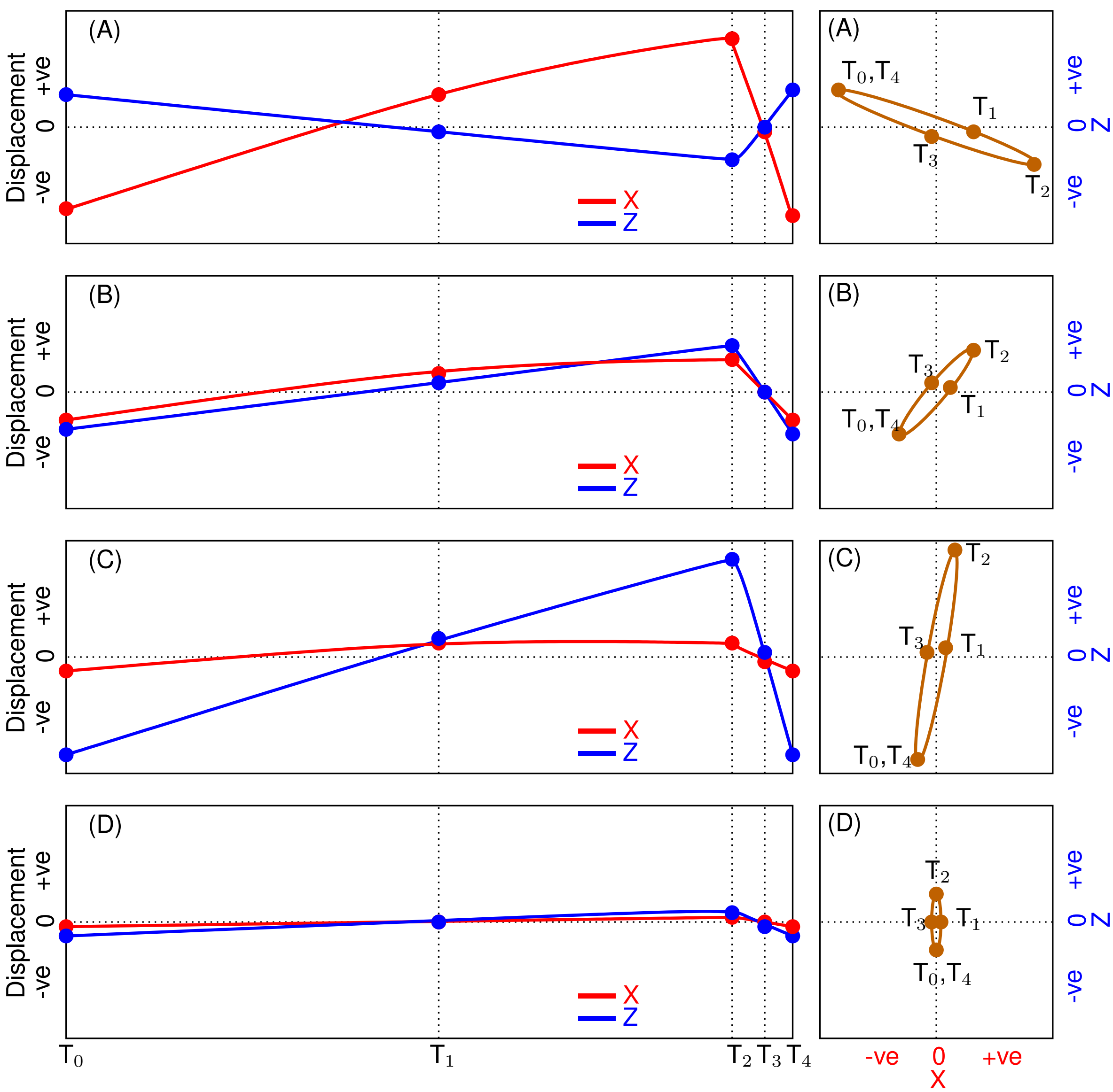

Figure A1: **Time-dependent detrended displacements (left column) and corresponding hodograms (right column) of points A through D (Figure2) during a single cycle of Episodic Buckling and Collapse.** Horizontal displacement X is shown in red and vertical displacement Z in blue. The different phases of the subduction cycle are also denoted.

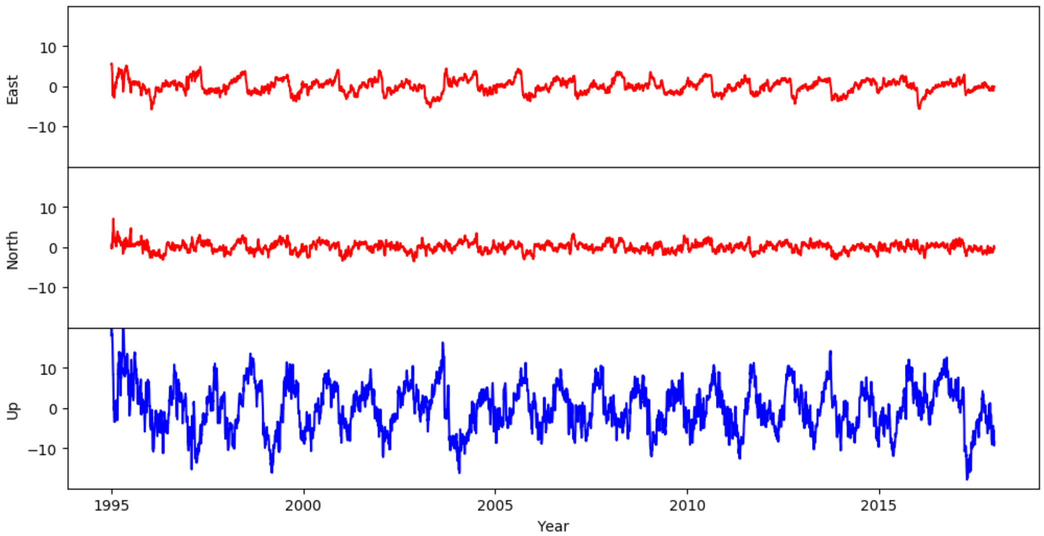

(a) GPS

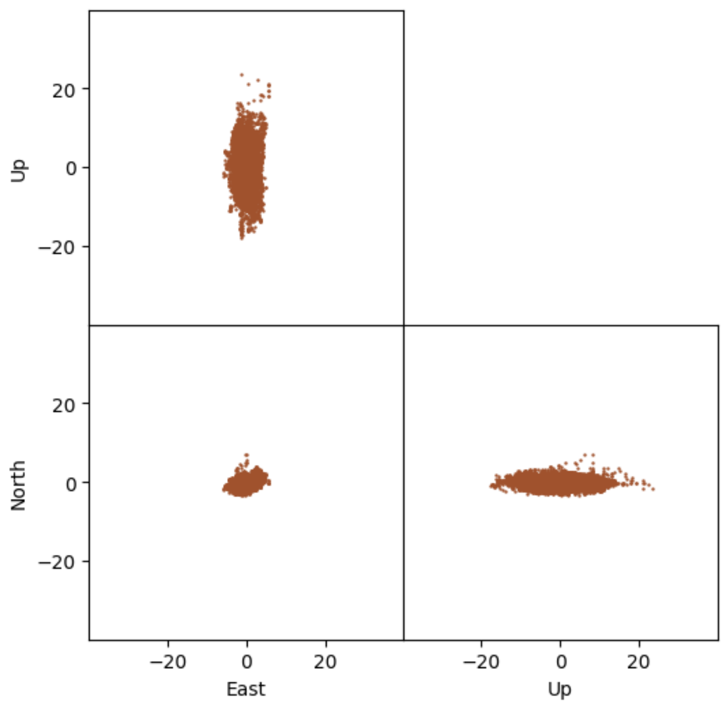

(b) Hodogram

Figure A2: **East, North, and vertical components of GPS data and corresponding hodogram from the Albert Head GPS site on Vancouver Island in Victoria, British Columbia and corresponding hodogram on the right.** All data have been detrended and filtered. The hodogram is displayed in the form of projections on the three orthogonal planes.

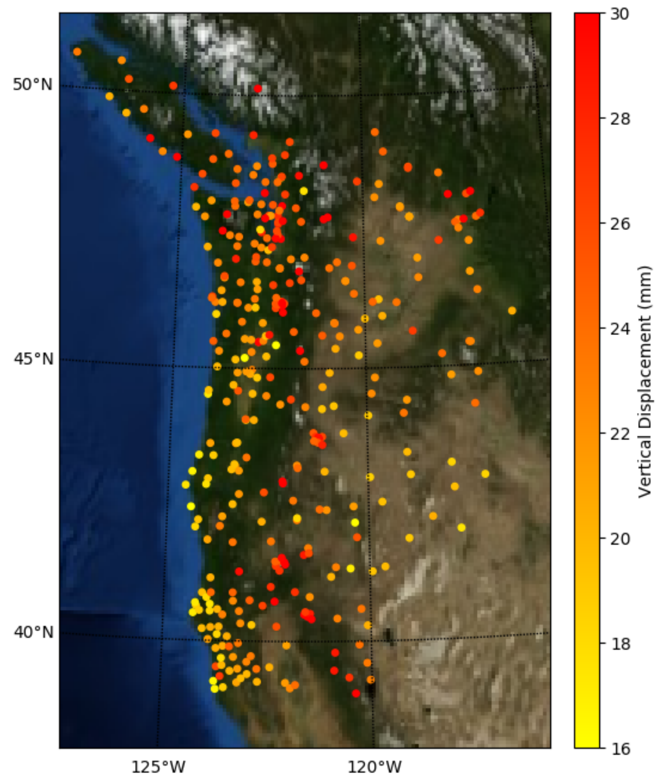

(a) Vertical displacement

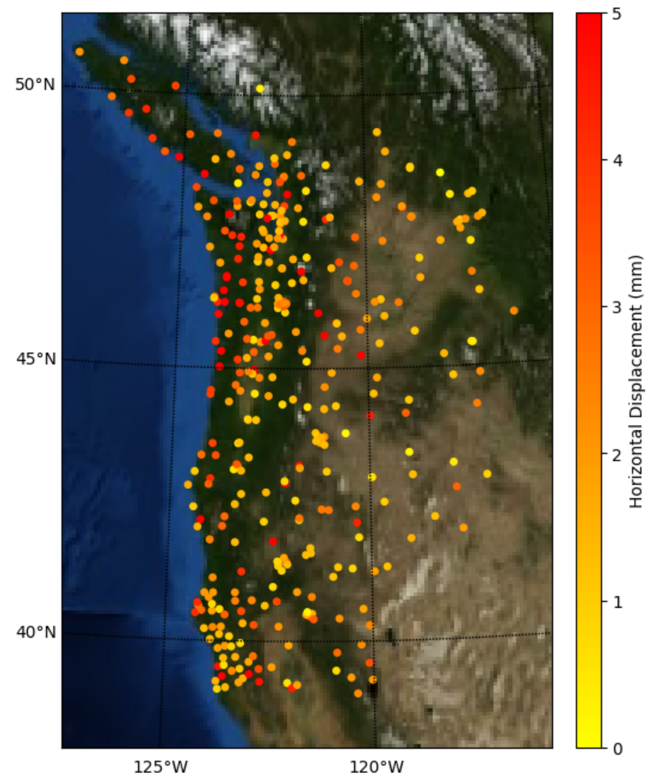

(b) Horizontal displacement

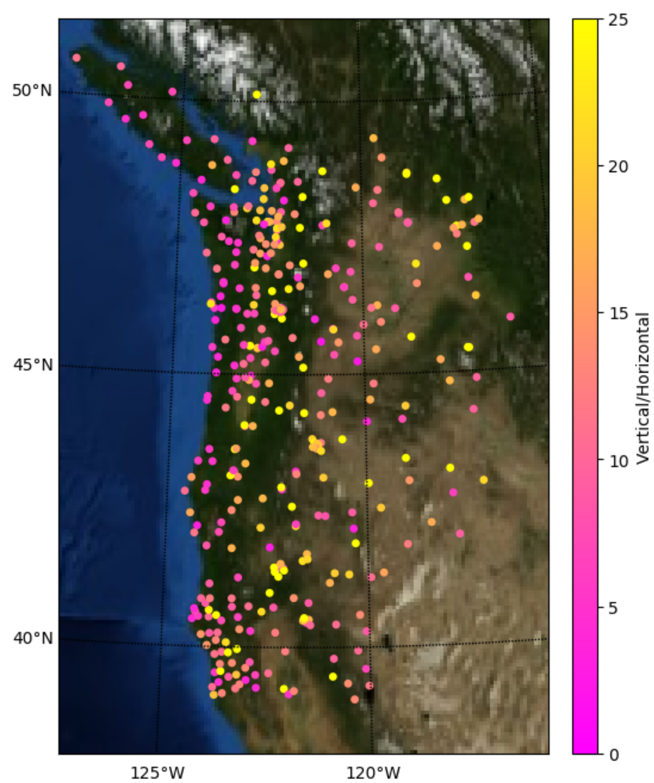

(c) Vertical-Horizontal Ratio

Figure A3: **Measures of surface deformation in Cascadia subduction zone. a,** Net vertical displacement and **b,** net horizontal displacement computed from GPS measurements, and **c,** their ratio. All color scales have been truncated to expose the patterns.

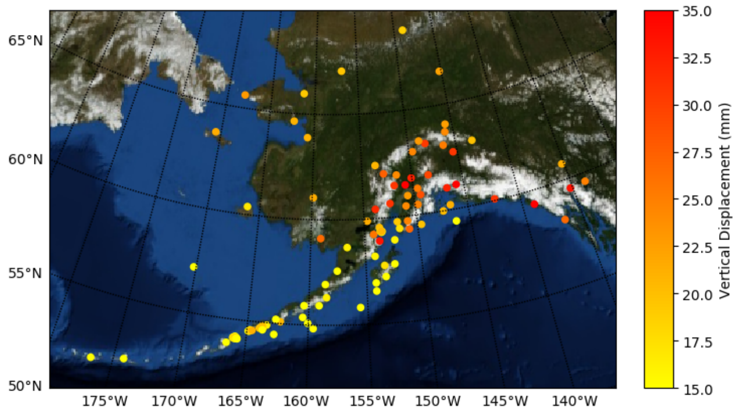

(a) Vertical displacement

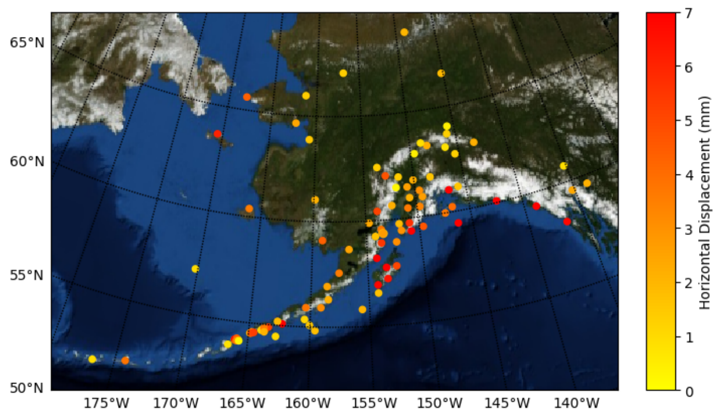

(b) Horizontal displacement

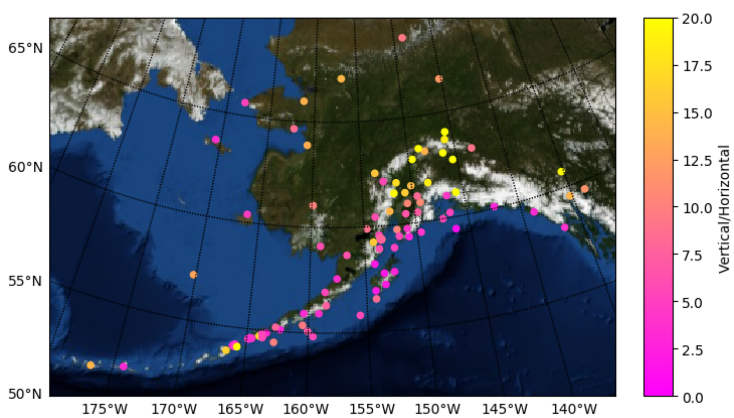

(c) Vertical-Horizontal Ratio

Figure A4: **Measures of surface deformation in Alaska. a,** Net vertical displacement and **b,** net horizontal displacement computed from GPS measurements, and **c,** their ratio. All color scales have been truncated to expose the patterns.